An extended x-ray absorption fine structure study of hydrogen storage in Ti–Hf–Ni alloys

2003 J. Phys.: Condens. Matter 15 7469

(http://iopscience.iop.org/0953-8984/15/44/003)

INSTITUTE OF PHYSICS PUBLISHING JOURNAL OF PHYSICS: CONDENSED MATTER

J. Phys.: Condens. Matter **15** (2003) 7469–7479 PII: S0953-8984(03)64310-9

An extended x-ray absorption fine structure study of hydrogen storage in Ti–Hf–Ni alloys

A Sadoc[1,2], V T Huett[3] and K F Kelton[3]

[1] Laboratoire de Physique des Matériaux et des Surfaces, Université de Cergy-Pontoise, Neuville sur Oise, 95031 Cergy-Pontoise Cedex, France
[2] Laboratoire pour l'Utilisation du Rayonnement Electromagnétique, CNRS, MENESR, CEA, Bâtiment 209D, Centre Universitaire Paris-Sud, BP 34, 91898 Orsay Cedex, France
[3] Department of Physics, Washington University, St Louis, MO 63130, USA

E-mail: Anne.Sadoc@lpms.u-cergy.fr

Received 3 June 2003
Published 24 October 2003
Online at stacks.iop.org/JPhysCM/15/7469

Abstract

The effect of hydrogenation on the local structure of a $Ti_{40}Hf_{40}Ni_{20}$ crystalline alloy was studied by means of the extended x-ray absorption fine structure. The samples were loaded to different hydrogen-to-metal ratios, H/M, between 1.2 and 1.7. The desorption process was also investigated by studying the local order in an alloy charged to $H/M = 1.85$ then desorbed to $H/M = 0.8$. For the non-hydrogenated alloys, the local order was very similar in Ti–Hf–Ni and Ti–Zr–Ni alloys, quasicrystal or crystal. With increasing hydrogen concentration, all of the mean interatomic distances increased, except for the Ni–Hf (Hf–Ni) ones, which show an anomalous behaviour, decreasing with increasing H/M. This leads to a remarkable inversion of the atomic subshells of titanium and nickel in the first environment of hafnium atoms around $H/M = 1.2$. The increase of distances is a maximum for the Ti–Ti and the Ti–Hf correlations, which is consistent with the hydrogen atoms sitting preferentially near titanium and hafnium atoms. Similar conclusions were obtained previously from a study of Ti–Zr–Ni alloys.

(Some figures in this article are in colour only in the electronic version)

1. Introduction

Ti-based quasicrystals and related crystals have a large capacity for hydrogen storage [1, 2]. In fact, the large number of tetrahedral sites in the structure, combined with the natural affinity of Ti and Zr atoms for hydrogen, makes the Ti–Zr–Ni quasicrystalline phase a possible candidate for constitutive materials in hydrogen batteries. The phase can absorb up to two hydrogen atoms for each metallic atom at about 350 °C [3]. Very recently, it has been shown that a $Ti_{40}Hf_{40}Ni_{20}$ alloy, a 3/2 cubic rational approximant phase, absorbs hydrogen to similar

levels as in icosahedral Ti–Zr–Ni, at lower temperature, 250 °C. Approximants are crystalline phases related to quasicrystals. The p/q cubic approximants of a given quasicrystal follow a Fibonacci sequence of rational fractions, p/q, ever closer to the golden mean, $\tau = (1+\sqrt{5})/2$. Unlike Ti–Zr–Ni, however, the formation of an irreversible hydride phase is suppressed in $Ti_{40}Hf_{40}Ni_{20}$ [4]. This makes this new phase a more promising hydrogen storage material or, at least, due to the heavy hafnium atoms involved and their high cost, it can be used as a test case for developing new materials at low loading temperature.

The effect of hydrogenation on the local structure has been studied by means of extended x-ray absorption fine structure (EXAFS) in Ti–Zr–Ni alloys [5, 6], quasicrystals and approximants. Although EXAFS, like x-ray diffraction (XRD), is not directly sensitive to the presence of light elements such as hydrogen, it does allow the study of the average change in local order induced by the introduction of hydrogen, with the Ti, Zr and Ni atoms acting like spy atoms. A general increase in all of the mean interatomic distances was obtained with increasing hydrogen concentration, except for the Ni–Zr (Zr–Ni) one, which decreased. The increase of the Zr–Ti correlation, together with the decrease of the Zr–Ni one, results in a remarkable inversion of the atomic subshells of titanium and nickel around zirconium at an H/M ratio around 1. As the interatomic distances do not change equally upon hydrogenation, hydrogenation does not only produce an expansion of the (quasi)crystal lattice, as would be inferred from the monotonic increase of the lattice parameter determined by XRD.

This evolution of interatomic distances in the Ti–Zr–Ni phases is rather astonishing. Moreover, the modification of the local structure with hydrogenation can provide important clues about how hydrogen absorption changes the local structure and how the desorption can proceed. Therefore, it is of interest to determine the local order to understand the experimental conditions under which hydrogen can be stored. To investigate this further, we have undertaken an EXAFS study of the evolution of the short range ordering as a function of the hydrogen concentration in the related 3/2 Ti–Hf–Ni alloy. Moreover, we also attempt to better understand the hydrogenation–dehydrogenation process in these Ti–Hf–Ni alloys by studying an alloy hydrogenated to H/M = 1.85, then desorbed to H/M = 0.8.

2. Experimental details

Samples of $Ti_{40}Hf_{40}Ni_{20}$, a 3/2 cubic rational approximant phase, were prepared and characterized at Washington University [4]. Alloy ingots of the desired composition were first produced by arc-melting mixtures of the pure elements on a water-cooled copper hearth in a high purity argon gas atmosphere. These ingots were subsequently melted and quenched in an argon atmosphere onto a rotating copper wheel to produce ribbons. The samples were loaded at 250 °C with hydrogen from the gas phase to H/M = 1.2, 1.4 and 1.7. In the following discussion, the non-hydrogenated sample will be designated as '3/2' and the hydrogenated ones as '3/2 + H/M'. Gas-phase hydrogenation studies were made using a computer-controlled modified Sievert's apparatus. The values of H/M were determined from the mass change. Prior to exposure to hydrogen, the samples were first plasma-etched in argon and coated with a thin layer of palladium (15–30 nm). The removal of the oxide layer by plasma-etching, followed by the vapour deposition of a thin layer of palladium, substantially enhances the rate of hydrogen absorption. The hydrogenation–dehydrogenation process was studied in a $Ti_{40}Hf_{40}Ni_{20}$ 3/2 approximant alloy hydrogenated to H/M = 1.85, then desorbed to H/M = 0.8. The hydrogen was desorbed by continual pumping with a turbo-molecular pump, holding the sample at a temperature of 250 °C for approximately 3 days. The phase purity of the samples was checked by XRD. Figure 1 shows the XRD patterns of the samples. The Bragg peaks shift to lower 2θ values when H/M increases. After desorption (H/M = 0.8), the position of the Bragg peaks

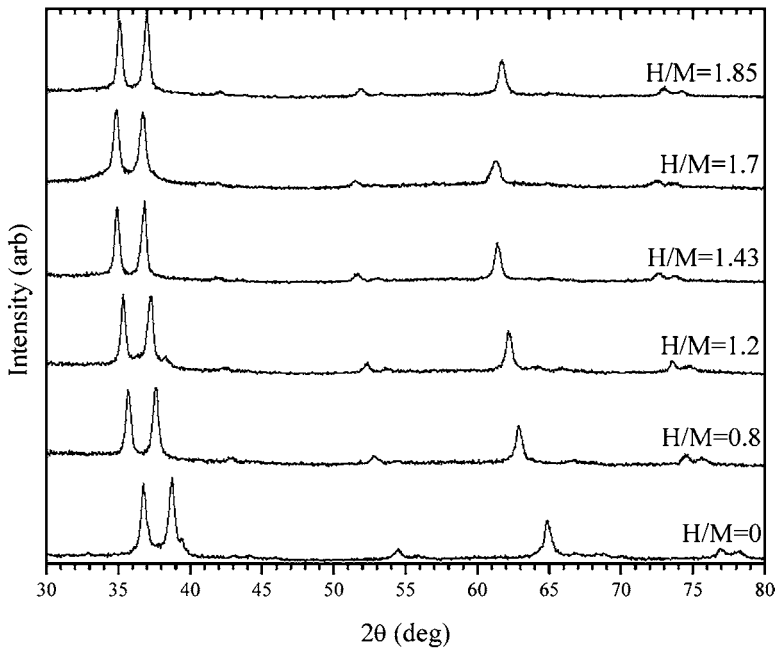

Figure 1. XRD patterns of the $Ti_{40}Hf_{40}Ni_{20}$ samples.

is intermediate between that for H/M = 0 and that for H/M = 1.2. The XRD pattern for H/M = 0 exhibits a small peak at around 39.5°. This is due to the Ti_2Ni-type phase [4]. It also shows up for H/M = 1.2 but has shifted with hydrogenation. This small amount of minority phase actually was destabilized by the hydrogenation, so in samples above H/M = 1.2 it has disappeared, and did not return after desorption, as in the sample with H/M = 0.8. In any case, this phase was in too small an amount to affect the EXAFS results. The widths of the Bragg peaks are almost constant with hydrogenation, apart for H/M = 1.7 for which some broadening of the (101000) peak (at around 65°) appears. However, the XRD patterns were performed on powder samples, which did not allow a detailed study of the disorder in the samples, due to a variation in powder size and possible strain introduced in crushing the samples.

The EXAFS experiments were performed on powdered samples sieved below 50 μm. They were carried out at the Laboratoire pour l'Utilisation du Rayonnement Electromagnétique (LURE, Orsay) using the DCI synchrotron radiation facility on the experimental station EXAFS 13. The x-ray absorption spectra at the Ti and Ni K edges and Hf L_{III} edge (4966, 8331 and 9560 eV respectively) were collected in transmission mode, at low temperature (10 K) using an Si 111 or Si 331 double-crystal monochromator or channel-cut single-crystal monochromator. The intensity of the beam before (I_0) and after (I) the sample was measured with ionisation chambers filled with air. For reference samples and for energy calibration of the EXAFS apparatus, titanium, nickel and hafnium foils were used.

3. EXAFS results

Standard procedures of normalization and background removal were followed to determine the EXAFS oscillations, χ, versus the energy, E, of the photoelectron from the absorption

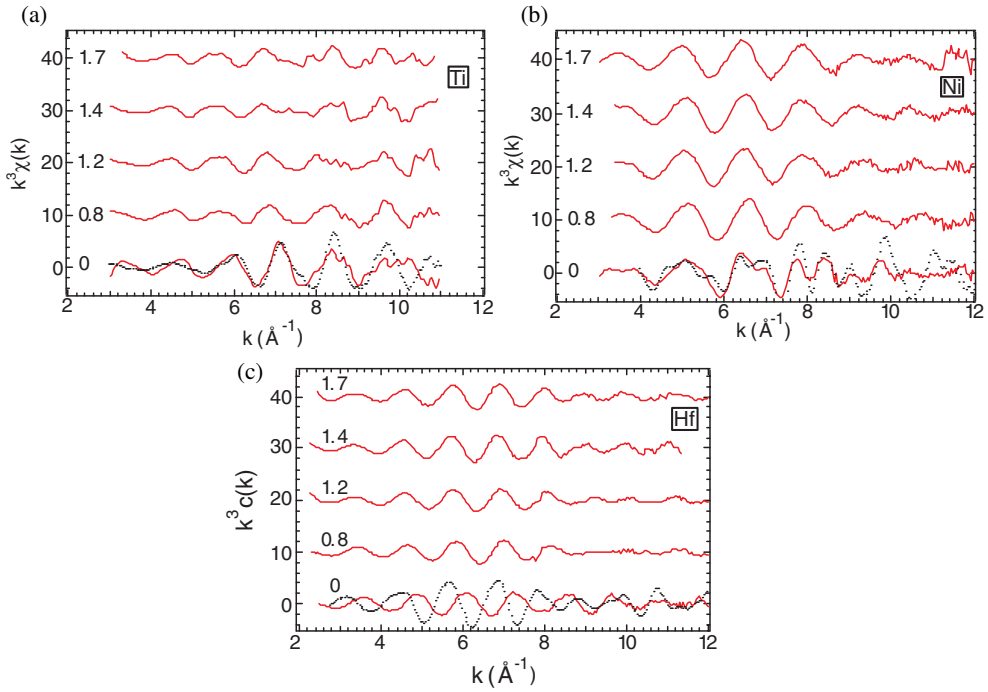

Figure 2. The EXAFS spectra, $k^3\chi(k)$, of the $Ti_{40}Hf_{40}Ni_{20}$ samples loaded to H/M = 0, 0.8 (desorbed sample), 1.2, 1.4 and 1.7 (solid curve). From (a)–(c): Ti K edge, Ni K edge, Hf L_{III} edge. For H/M = 0, comparison is made with the Ti, Ni and Zr K edges of 1/1 Ti–Zr–Ni (dots).

coefficient, $\ln I_0/I$, using a program package [7, 8]. The data were then converted to k-space using $\hbar^2k^2/2m = E - E_0$, where E_0 is the threshold energy origin. The normalized EXAFS signals, $k^3\chi(k)$, are compared, for the different samples, in figure 2 for the Ti, Ni and Hf edges. Spectra obtained previously [5, 6] for the non-hydrogenated 1/1 Ti–Zr–Ni sample are also shown.

The spectra of the hydrogenated samples look very different from those of the non-hydrogenated one, even for the less hydrogenated sample (the desorbed sample, H/M = 0.8); this is particularly evident for the Ni edge. There is a general tendency for the EXAFS oscillations to be smaller in the hydrogenated samples. Moreover, they shift to lower k-values when H/M increases, according to the simple idea that the interatomic distances increase together with the lattice parameter. Comparing the non-hydrogenated Ti–Hf–Ni and Ti–Zr–Ni alloys, the spectra look very similar for the Ti edge and for the Ni edge, with a somewhat smaller intensity for Ti–Hf–Ni. Consequently, the local order must be similar in both alloys, at least around the titanium and nickel atoms, and perhaps a little more disordered in Ti–Hf–Ni. For the Hf L_{III} edge and Zr K edge, the spectra are almost of opposite phase. We will see in the following that this is not due to a different local order between the alloys, but to a different phase shift experienced by the photoelectron when absorbed by hafnium or zirconium atoms.

The Fourier transforms (FTs) of these data for $k^3\chi(k)$ were obtained within a k window from roughly 3 to 12 $Å^{-1}$ for the Ni and Hf edges and from 3 to 10 $Å^{-1}$ for the Ti edge, where the signal is noisy. The moduli of the FTs (figure 3) are qualitatively similar to the radial distributions of the atoms neighbouring the absorbing atom (Ti, Ni or Hf). However, the peaks are shifted to lower R-distances, because of the phase shifts experienced by the photoelectron

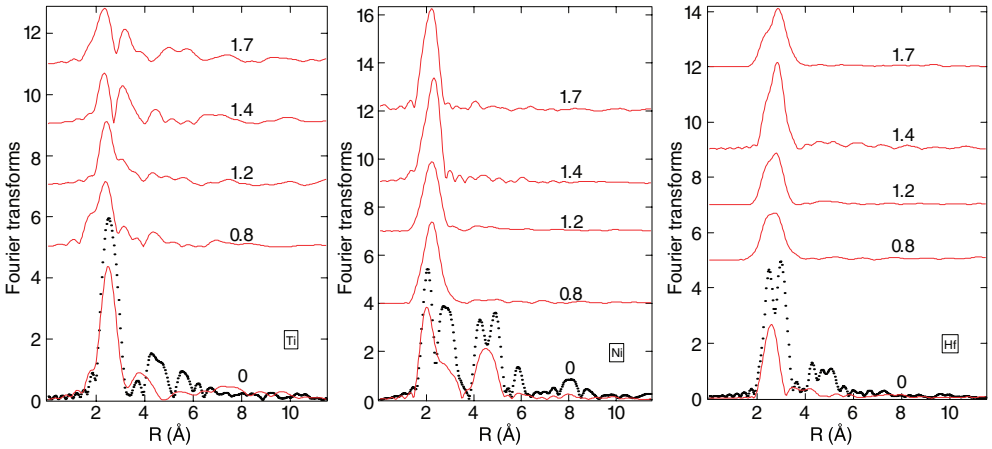

Figure 3. Moduli of the FTs of the $k^3\chi(k)$ as a function of distance (Å) in the $Ti_{40}Hf_{40}Ni_{20}$ alloys. From left to right: Ti K edge, Ni K edge, Hf L_{III} edge. For $H/M = 0$, comparison is made with the Ti, Ni and Zr K edges of 1/1 Ti–Zr–Ni (dots).

while scattering from the potentials of the absorbing atom and nearest neighbours. Due to these phase shifts, the shape of the modulus of the FT does not provide a simple explanation of the environments of the atoms or an interpretation of the evolutions of these environments. Simulations must be done.

The FTs show drastic differences between the non-hydrogenated alloy and the hydrogenated ones, although the XRD patterns always show the same Bragg peaks. The FTs are composed primarily of peaks of the first neighbours (1.5–4 Å range), but peaks of second neighbours clearly appear in the 4–5 Å region at the Ni edge in the non-hydrogenated alloy. After hydrogenation, this broad band in the 4–5 Å region (i.e. medium-range order) decreases significantly, or even disappears, which may indicate the development of a more disordered structure. This cannot be related to the disappearing of the Ti_2Ni phase, since this phase does still exist for $H/M = 1.2$, while no peaks of second neighbours appear in any of the FTs for this hydrogen content. At this Ni edge, the peak of first neighbours is doubly composed with a well-defined component centred at 2 Å (uncorrected for phase shift) and a broad and weaker shoulder from 2.5 to 3.5 Å. After hydrogenation, only the main peak survives, shifted towards higher-R values. At the Ti and Hf edges, the first-neighbour peak is centred at about 2.5 Å in the non-hydrogenated alloy. At the Hf edge, the main peak broadens with hydrogenation and, for $H/M = 1.7$, becomes a double peak, with the main component at about 2.9 Å, and a shoulder at lower R-values. At the Ti edge, this main peak shifts to lower R-values, while a smaller component appears at higher R-values. Comparing now the FTs of the non-hydrogenated 3/2 TiHfNi and the 1/1 TiZrNi alloys, similar features appear at the Ti and Ni edges. However,

- at the Ti edge, the main peak is less intense in the TiHfNi sample and there is no second neighbour peak above 4 Å;
- at the Ni edge, again the peak at 2 Å and the broad shoulder between 2.5 and 3.5 Å are less intense in the 3/2 sample;
- at the Hf edge, due to different phase shifts, the double first-neighbour peak in the TiZrNi sample corresponds here, in the TiHfNi one, to a unique peak, which is again less intense.

To determine the first coordination shell around Ti, Ni or Hf atoms in the different samples, the first peaks between roughly 1.5 and 3.5 Å were back-transformed to k-space. These Fourier-filtered spectra were fit using the following formula [9], which in single scattering theories, describes the EXAFS oscillations for a Gaussian distribution of neighbours around a central atom:

$$\chi(k) = -\sum_j \frac{N_j}{kR_j^2} B_j(k) \exp\left(-2\sigma_j^2 k^2 - \frac{2R_j}{\lambda}\right) \sin(2kR_j + 2\delta_1' + \phi_j(k)). \quad (1)$$

The sum is taken over shells with N_j atoms at distances R_j from the absorbing atom. σ_j is the mean square relative displacement of absorber and j backscatter atoms, so that the Debye–Waller factor $\exp(-2\sigma_j^2 k^2)$ is a measure of both static and dynamic disorder in shell j. It arises mainly from structural disorder, since the experiments were mostly made at low temperature. $B_j(k)$ and $\phi_j(k)$ are the backscattering amplitude and the phase shift, respectively, experienced by the photoelectron while scattering by the neighbours; δ_1' is the phase shift of the central atom and λ is the electron mean free path. The amplitudes and phase shifts were taken from McKale *et al* [10]. The fitting of the first-neighbour peak in the FT was performed in both k- and R-space.

Since the Ti and Ni spectra look very similar for the 1/1 TiZrNi and 3/2 TiHfNi alloys, a structural model of the 1/1 approximant TiZrNi phase (W phase) [11] was used to analyse the EXAFS spectra of the TiHfNi 3/2 approximant, even around the hafnium atom. Then, the local structure of the hydrogenated TiHfNi alloys was derived from that of the 3/2 approximant TiHfNi phase.

4. Structural modelling of 1/1 Ti–Zr–Ni and 3/2 Ti–Hf–Ni approximant phases

The refined structure of the W phase (1/1 approximant) of the Ti–Zr–Ni phase was based on x-ray and neutron diffraction measurements [12] and *ab initio* calculations [11]. The basic cluster is a Bergman-type cluster, with the centre occupied by a nickel atom. The nickel atom is surrounded by 12 titanium atoms, giving a nearly undistorted icosahedron. A larger, second-shell, icosahedron contains 12 titanium/zirconium atoms. The numbers and average distances of nearest neighbours are summarized in table 1. All distributions of distances are broad. Around a titanium or a zirconium atom, there are nickel, titanium and zirconium neighbours. Around nickel, there are, on an average, 2.8 titanium first neighbours (Ti 1) located at a well-defined distance of 2.44 Å and 2.8 titanium atoms (Ti 2) at a mean distance of 2.73 Å, plus a few more zirconium neighbours at distances beyond 3 Å. Most average interatomic distances have values near the sum of the atomic radii (Ti: 1.47 Å, Zr: 1.60 Å, Ni: 1.24 Å). However, the first Ti–Ni correlation, 2.44 Å, is clearly shorter than the sum of the atomic radii of Ti and Ni (2.71 Å). Also, the Zr–Ni (Ni–Zr) mean distance, 3.19 Å, is greater than the sum of the atomic radii of Zr and Ni (2.84 Å).

EXAFS spectra of this 1/1 Ti–Zr–Ni phase were obtained previously and successfully described based on this atomic model [5]. The average distances determined by EXAFS differ by less than 0.10 Å from the diffraction results. It should be kept in mind that the distributions of distances are very broad in the 1/1 phase, which does not allow a precise determination of the distances by EXAFS. The error bars were taken to be $\Delta R = \pm 0.06$ Å and $\Delta\sigma = \pm 0.06$ Å. It is however difficult to estimate the uncertainties, even for distances. On the one hand, some interference effect can be obtained only within ± 0.005 Å; on the other hand, the distributions of distances are broad. The same values of the interatomic distances were recovered for the heterogeneous pairs, from different edges, within about ± 0.06 Å, which was taken to be the error bar for R and σ.

Table 1. First environments in 1/1 $Ti_{50}Zr_{35}Ni_{15}$ and in 3/2 Å $Ti_{40}Hf_{40}Ni_{20}$ alloys. For the EXAFS data, $\Delta R = \pm 0.06$ Å and $\Delta\sigma = \pm 0.06$ Å.

			1/1 $Ti_{50}Zr_{35}Ni_{15}$			3/2 $Ti_{40}Hf_{40}Ni_{20}$	
			Diffraction [8]	EXAFS [4]		EXAFS	
Central atom	$\bar{N}$		$\bar{R}$ (Å)	R (Å)	σ (Å)	R (Å)	σ (Å)
Ti	1	Ni 1	2.44	2.45	0.105	2.48	0.11
	1	Ni 2	2.73	2.82	0.08	2.78	0.07
	4.9	Ti	2.90	2.85	0.18	2.90	0.21
	5.1	Zr/Hf	3.07	3.02	0.12	3.01	0.12
Ni	2.8	Ti 1	2.44	2.46	0.085	2.49	0.11
	2.8	Ti 2	2.73	2.70	0.09	2.68	0.13
	5.6	Zr/Hf	3.19	3.15	0.11	3.19	0.14
Zr/Hf	8	Ti	3.07	3.05	0.12	3.05	0.11
	2.75	Ni	3.19	3.25	0.09	3.24	0.11
	4.5	Zr/Hf	3.27	3.33	0.10	3.35	0.18

This structural modelling of the 1/1 Ti–Zr–Ni phase was used to simulate the EXAFS spectra of the 3/2 Ti–Hf–Ni phase, substituting zirconium by hafnium. The number, N, of nearest neighbours was fixed to the values found in the model of the 1/1 phase, while the distances, R, and the disorder parameter, σ, were adjusted to fit the calculated spectra to the experimental data (table 1). Good reconstruction of the EXAFS spectra could be done, especially at the Hf edge, where the EXAFS spectrum is almost out of phase with that of Ti–Zr–Ni at the Zr edge. As a matter of fact, there is a difference of near $3\pi + \frac{\pi}{4}$, in the 4–8 $Å^{-1}$ region, between the phase shifts, $2\delta_1'$, for hafnium and zirconium photo-absorber atoms. Therefore, for a similar environment (coordination number, distances, etc), a phase shift appears between the two spectra, which look almost opposite in phase ($\pi + \frac{\pi}{4}$).

Based on the near-average distances that were found, the local structure is very similar in the 1/1 Ti–Zr–Ni and 3/2 Ti–Hf–Ni phases, even around the zirconium/hafnium atoms. Therefore, the model of the 1/1 Ti–Zr–Ni phase was used to reconstruct the spectra of the hydrogenated Ti–Hf–Ni alloys.

5. Hydrogenation/dehydrogenation

To simulate the spectra of the hydrogenated Ti–Hf–Ni alloys from the 1/1 model, the number, N, of nearest neighbours was kept constant, assuming that the mean coordination numbers remain unchanged upon hydrogenation. The distances, R, and the disorder parameter, σ, were allowed to vary. The fitting of the hydrogenated alloys was performed, going from the R and disorder values found for the non-hydrogenated alloy, in more and more hydrogenated alloys. Therefore, only small changes of R and σ were allowed from one hydrogenated sample to a more hydrogenated one. Moreover, the parameters had to be consistent for the heterogeneous pairs (for example Ti–Hf and Hf–Ti, etc). This also restricted drastically the values of the parameters. The values used to fit the spectra are given in table 2. The σ-parameters have nearly the same values with no discernable correlation with H/M. The distances obtained for the sample hydrogenated to H/M = 1.85, then desorbed to 0.8, are intermediate between those for the non-hydrogenated alloy and those for the 3/2, with an H/M of 1.2. Therefore, the absorption/desorption process appears to be reversible, at least up to H/M = 0.8. Moreover,

Table 2. First environments in 3/2 Ti–Hf–Ni + H/M alloys. $\Delta R = \pm 0.06$ Å and $\Delta\sigma = \pm 0.06$ Å.

H/M			0		0.8		1.2		1.4		1.7	
Central atom	$\bar{N}$		R (Å)	σ (Å)	R (Å)	σ (Å)	R (Å)	σ (Å)	R (Å)	σ (Å)	R (Å)	σ (Å)
Ti	1	Ni	2.48	0.11	2.50	0.07	2.60	0.11	2.55	0.12	2.55	0.13
	1	Ni	2.78	0.07	2.73	0.08	2.84	0.06	2.82	0.08	2.84	0.08
	4.9	Ti	2.90	0.21	2.99	0.19	3.10	0.21	2.97	0.20	3.07	0.22
	5.1	Hf	3.01	0.12	3.05	0.15	3.14	0.12	3.23	0.14	3.19	0.14
Ni	2.8	Ti	2.49	0.11	2.54	0.10	2.55	0.10	2.58	0.11	2.59	0.11
	2.8	Ti	2.68	0.13	2.70	0.22	2.80	0.23	2.90	0.23	2.75	0.21
	5.6	Hf	3.19	0.14	3.17	0.20	3.24	0.22	3.15	0.22	3.15	0.24
Hf	8	Ti	3.05	0.11	3.05	0.12	3.08	0.13	3.23	0.10	3.23	0.11
	2.75	Ni	3.24	0.11	3.16	0.10	3.18	0.10	3.02	0.09	3.01	0.12
	4.5	Hf	3.35	0.18	3.37	0.13	3.43	0.14	3.46	0.20	3.40	0.14

the desorbed sample could be treated as a sample that was hydrogenated to an H/M of 0.8, at least to follow the evolution of the distances with hydrogenation. The values of the disorder parameter are very near before (H/M = 1.2) and after desorption. The distances are plotted in figure 4 versus H/M for all of the correlations. The lines are guides for the eye. One can notice the following.

- In agreement with the increase in the quasilattice constant measured by XRD, there is a general increase of all the mean distances, except however for the Hf–Ni (Ni–Hf) one. The increase of the Hf–Ti correlation and the decrease of the Hf–Ni one result in an inversion of these distances around H/M = 1.2, indicating an inversion of the titanium and nickel atomic subshells in the environment of hafnium atoms.
- The increase is a maximum for the Ti–Hf and the Ti–Ti correlations. Therefore, it can be concluded that the perturbation of the lattice due to hydrogenation is also a maximum around the titanium and hafnium atoms and, consequently, that hydrogen atoms sit preferentially near titanium and hafnium neighbours.

These same conclusions were obtained from the study of hydrogenation in Ti–Zr–Ni alloys [6]. Therefore, this could signal a general behaviour, at least for this type of sample. In Ti–Zr–Ni, the location of hydrogen near Ti and Zr atoms, consistent with the natural affinity of Ti and Zr atoms for hydrogen, was obtained not only from EXAFS measurements, but also from nuclear magnetic resonance studies [13] and from experimental investigations of the valence and conduction bands [14].

To advance our understanding of the hydrogenation, it is necessary to explain the decrease of some distances. A foundation for an interpretation could lie in a comparison of the atomic radii. In the non-hydrogenated 3/2 phase, the Hf–Ni distance (3.21 Å) is larger than the sum (2.82 Å) of the atomic radii of Hf and Ni (Hf: 1.58 Å, Ni: 1.24 Å). As a consequence, the Hf–Ni correlations could be more easily reduced upon hydrogenation, the corresponding Hf and Ni atoms being displaced from their ideal positions. The same holds true for Ti–Zr–Ni. In most transition metal alloys, hydrogen atoms prefer to sit in tetrahedrally coordinated sites. Icosahedral quasicrystals, as well as their crystalline approximants, are likely dominated by local tetrahedral order and thus provide a variety of sites for interstitial hydrogen. The expansion of the interstitial tetrahedral sites, occupied by hydrogen, could push the hafnium/zirconium toward nickel neighbours, causing a decrease in the corresponding interatomic distances.

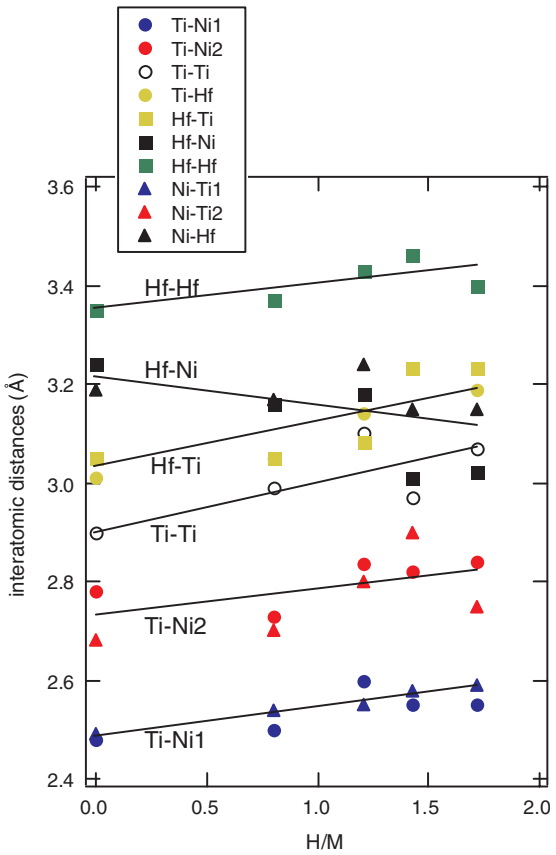

Figure 4. First interatomic distances versus H/M. The lines are guides for the eye.

The introduction of hydrogen in the lattice induces, therefore, not only an expansion of the lattice, but can also bring some atoms closer together. As the changes in the distances are not the same for all types of atoms, although the lattice parameter increases linearly, the structure of the hydrogenated alloys is not a simple dilatation of that of the non-hydrogenated one. Moreover, the different changes in the distances would likely cause large distortions in the local structure, possibly reflected by the vanishing of the second neighbourhood in the FTs. During the desorption process, the lattice is shrinking and the exchange of titanium and nickel atoms in the environment of hafnium atoms would likely become more difficult, possibly explaining the difficulties in desorbing the samples. Therefore, the desorption process could be easily reversible up to about $H/M = 1$. To conclude about the important question of reversibility, the hydrogenation is clearly not reversible for the non-hydrogenated sample since the Ti_2Ni phase has disappeared above $H/M = 1.2$ and did not return after desorption, as in the sample with $H/M = 0.8$. However, all the XRD and EXAFS results show that the hydrogenation is fully reversible for the 3/2 Ti–Hf–Ni phase, at least for dehydrogenation up to $H/M = 0.8$.

A two-step hydrogenation process has recently been proposed to interpret the hydriding properties of mechanically alloyed icosahedral Ti–Zr–Ni alloys [15]. The authors assume the existence of at least two kinds of hydrogen sites in the structure. The hydrogen atoms of the first type would occupy some tetrahedral sites within the Bergman clusters, while those of the second

type would occupy the sites in the regions between the Bergman clusters. Upon hydrogenation, hydrogen would start to fill the tetrahedral positions inside the Bergman clusters. The filling of these positions would proceed up to a hydrogen content of about $H/M = 1.1$, for which all the positions would be occupied. For higher H/M, hydrogen starts to fill the sites between the Bergman clusters. It is worth noting that the transition between these two stages occurs at the same H/M value as the inversion of the titanium and nickel atomic subshells in the environment of hafnium/zirconium atoms.

6. Conclusions

EXAFS measurements were made in order to study the influence of hydrogen on the local structure of the Ti–Hf–Ni alloys, 3/2 approximants, and to compare the behaviour to that found previously in Ti–Zr–Ni alloys, quasicrystals and 1/1 approximants. Hydrogen concentrations of $H/M = 1.2$, 1.4 and 1.7 were studied and the dehydrogenation process was investigated in an alloy loaded to $H/M = 1.85$, then desorbed to 0.8. For the non-hydrogenated alloys, the local order was very similar in the 3/2 Ti–Hf–Ni and 1/1 Ti–Zr–Ni alloys and the EXAFS spectra of the Ti–Hf–Ni alloy could be reconstructed using a model for the 1/1 Ti–Zr–Ni alloy. This model was then used to determine the evolution of the local structure with hydrogenation. The distances obtained for the sample hydrogenated to $H/M = 1.85$ then desorbed to 0.8 are intermediate between those for the non-hydrogenated alloy ($H/M = 0$) and those for $H/M = 1.2$. Therefore, the changes in the interatomic distances and, consequently, in the local structure, appear reversible for 3/2 Ti–Hf–Ni. As in Ti–Zr–Ni, all the mean interatomic distances were found to increase with increasing hydrogen content, except for the Hf–Ni (Zr–Ni) ones, which show an anomalous behaviour, decreasing with increasing H/M. As the increase of distances is a maximum for the Ti–Ti and the Ti–Hf (Ti–Zr) correlations, the perturbation of the lattice due to hydrogenation is also a maximum around titanium and hafnium (zirconium) atoms. Therefore, it can be concluded that hydrogen atoms sit preferentially near titanium and hafnium (zirconium) atoms, confirming previous results of studies of hydrogenated Ti–Zr–Ni alloys. The increase of the Hf–Ti correlation together with the decrease of the Hf–Ni one results in a remarkable inversion of the atomic subshells of titanium and nickel around hafnium for an H/M ratio around 1.2. During the desorption process, the lattice is shrinking and the exchange of titanium and nickel atoms would likely become more difficult, possibly explaining the difficulties in desorbing the samples. The hydrogenation process appears to be of a very complex nature, leading to a reorganization of the local structure, but leaving the long range structure unchanged.

Acknowledgments

We are pleased to thank our colleagues J Moscovici and A Traverse for their help during the EXAFS experiments. K F Kelton gratefully acknowledges the support of the National Science Foundation under grant DMR 00-72787.

References

[1] Kelton K F, Kim W J and Stroud R M 1997 *Appl. Phys. Lett.* **70** 3230
[2] Kelton K F and Gibbons P C 1997 *Mater. Res. Soc. Bull.* **22** 69
[3] Viano A M, Stroud R M, Gibbons P C, McDowell A F, Conradi M S and Kelton K F 1995 *Phys. Rev.* B **51** 12026
[4] Huett V T and Kelton K F 2002 *Phil. Mag. Lett.* **82** 191

[5] Sadoc A, Kim J Y and Kelton K F 2001 *Phil. Mag.* A **81** 2911
[6] Sadoc A, Majzoub E H, Huett V T and Kelton K F 2002 *J. Phys.: Condens. Matter* **14** 6413
[7] Michalowicz A 1991 EXAFS pour le MAC *Logiciels pour la Chimie* (Paris: Société Française de Chimie) p 102
[8] Michalowicz A 1997 *J. Physique Coll.* IV **7** C2 235
[9] Stern E A, Sayers D E and Lytle F W 1975 *Phys. Rev.* B **11** 4836
[10] McKale A G, Veal B W, Paulikas A P, Chan S K and Knapp G S 1988 *J. Am. Chem. Soc.* **110** 3763
[11] Hennig R G, Majzoub E H, Carlsson A E, Kelton K F, Henley C L, Misture S, Kresse G and Hafner J 2000 *Proc. 7th Int. Conf. on Quasicrystals* ed F Gähler, P Kramer, H-R Trebin and K Urban; *Mater. Sci. Eng.* A **294/295** 361
[12] Kim W J, Gibbons P C, Kelton K F and Yelon W B 1998 *Phys. Rev.* B **58** 2578
[13] Faust K R, Pfitsch D W, Stojanovich N A, McDowell A F, Adolphi N L, Majzoub E H, Kim J Y, Gibbons P C and Kelton K F 2000 *Phys. Rev.* B **62** 11444
[14] Belin-Ferré E, Hennig R G, Dankhazi Z, Sadoc A, Kim J Y and Kelton K F 2002 *J. Alloys Compounds* **342** 337
[15] Konstanchuk I G, Ivanov E Yu, Bokhonov B B and Boldyrev V V 2001 *J. Alloys Compounds* **319** 290